

$\mathcal{O}(\alpha_s\alpha_t)$ (non)decoupling effects within the top-sector of the MSSM

L. Mihaila and N. Zerf

Institut für Theoretische Physik, University of Heidelberg, 69117 Heidelberg, Germany

Abstract

In this paper we compute the $\mathcal{O}(\alpha_s\alpha_t)$ threshold corrections to the running strong coupling constant, the top-Yukawa coupling and the top-quark mass within the MSSM. These parameters present a non-decoupling behaviour with the supersymmetry scale M_{SUSY} . Our numerical analysis shows that the mixed QCD-Yukawa corrections can amount to few GeV for the running top-quark mass and range at the percent level for the top-Yukawa coupling.

PACS numbers: 11.30.Pb, 12.38.-t, 12.38.Bx, 12.10.Kt

1 Motivation

After the end of the LHC run I and the start of the LHC run II, the direct searches for supersymmetric particles remained unsuccessful, thus increasing the exclusion bounds for the supersymmetric mass scale towards the TeV range [1]. For the time being, it seems that if supersymmetry is realised in high energy physics the most likely scenario is the one where all SUSY particles are much heavier than the SM ones. For such a mass hierarchy (also called the “decoupling limit” [2]), it was shown [3] that the effects of the SUSY particles on many physical observables in the gauge and Higgs sectors scales like $M_{\text{EW}}^2/M_{\text{SUSY}}^2$. Therefore, for very heavy SUSY scales, deviations from the SM predictions for these observables will be very challenging to detect. In such a case, additional efforts both in theory and experiment are required to identify physical observables for which the power suppressed behaviour does not occur, or the decoupling limit is delayed by parametric enhancements like in the presence of large $\tan\beta$ values [4]. Prominent examples for this class of observables are the mass of the lightest Higgs boson and its self coupling in SUSY theories that receive radiative corrections increasing with the SUSY mass scale and mixing parameters.

In this paper we study the behaviour of the running top quark mass and Yukawa coupling in the decoupling limit of the MSSM. Although, the running parameters are not themselves observables, they can be related in perturbation theory with more physical parameters like for example effective charges in the MOM scheme [5] or short-distance

masses in MSR [6].¹ Under the decoupling limit we understand that all the superpartners, including the additional Higgs particles A, H^0, H^\pm , are much heavier than the SM particles. We assume here that the relation $M_{\text{SUSY}}, M_A \gg M_{\text{EW}}$ holds. The case for an intermediate Higgs sector ($M_{\text{SUSY}} \gg M_A \gg M_{\text{EW}}$), *i.e.* at intermediate energies the 2HDM is at work, was studied in detail in the literature [4]. Here, we consider the case for which the lightest Higgs boson behaves SM like and no additional particles have masses at intermediate energy scales.

As will be shown in the next sections, the non-decoupling effects for the running quark masses and Yukawa couplings increase logarithmically with the SUSY mass scale and have a polynomial dependence with maximal degree three on the mixing parameters in the squark sectors. From a phenomenological point of view, the non-decoupling effects are usually few times larger than the current accuracy on the bottom and top quark mass determinations [7–9]. For Yukawa couplings the effects are in the range of precision expected for a 100 TeV collider [10]. In order to keep the theoretical uncertainties well below the experimental accuracy, we consider here the two-loop radiative corrections of order $\mathcal{O}(\alpha_s^2, \alpha_s \alpha_t)$ induced by the strong and the top-Yukawa couplings, and neglect the bottom-Yukawa coupling except for scenarios with large $\tan\beta$ values. Here, we concentrate on the theoretical aspects and give some details of the calculation.

The outline of this paper is as follows: in the next section we describe briefly the computational framework and introduce our notation. In section 3 we provide analytical results for the decoupling coefficients and discuss their phenomenological implications in section 4. Our findings are summarized in section 5.

2 Framework

In the following, we assume that all the SM particles are much lighter than any superpartner. In this case, the physical phenomena at low energies can be described with an effective theory, called the SMEFT (see Ref. [11] for a recent review), containing six quark flavours and the light Higgs. At leading order in the heavy masses, the effective Lagrangian \mathcal{L}_{eff} can be written as a linear combination of operators constructed from the light degrees of freedom. We adopt here a “top-down” approach, in the sense that the Wilson coefficients of the operators will be computed in the full theory, *i.e.* MSSM for our specific calculation. For the study of the running quark masses and Yukawa couplings up to $\mathcal{O}(\alpha_s^2, \alpha_s \alpha_t)$ it is sufficient to study the following three operators [12]

$$\mathcal{L}_{\text{eff}} = \mathcal{L}_{\text{SM}}^{(6)} + \mathcal{L}_{\text{eff}}^h + \dots; \quad \mathcal{L}_{\text{eff}}^h = -\frac{h^{(0)}}{v^{(0)}} \left[C_1^0 \mathcal{O}_1^0 + \sum_{q=u,d,\dots} (C_{2q}^0 \mathcal{O}_{2q}^0 + C_{3q}^0 \mathcal{O}_{3q}^0) + \dots \right]. \quad (1)$$

Here $\mathcal{L}_{\text{SM}}^{(6)}$ denotes the usual SM Lagrangian with six active quark flavours but without the Yukawa sector. The latter is considered explicitly in $\mathcal{L}_{\text{eff}}^h$, that collects all interactions

¹Nevertheless, the explicit conversion of the running parameters to physical observables is beyond the scope of this paper.

with just one Higgs field. The ellipsis stand for the remaining higher-dimensional operators that we do not study here. The Wilson coefficients $C_i, i = 1, 2q, 3q$, parameterize the effects of the heavy particles and the superscript 0 labels bare quantities. The three operators relevant in our computation are defined as

$$\begin{aligned}\mathcal{O}_1^0 &= (G_{\mu,\nu}^{0,t,a})^2, \\ \mathcal{O}_{2q}^0 &= m_q^{0,t} \bar{q}^{0,t} q^{0,t}, \\ \mathcal{O}_{3q}^0 &= \bar{q}^{0,t} (i \not{D}^{0,t} - m_q^{0,t}) q^{0,t},\end{aligned}\tag{2}$$

where $G_{\mu,\nu}^{0,t,a}$ and $D_\mu^{0,t}$ are the gluon field strength tensor and the covariant derivative for quark fields, and the primes label the quantities in the effective theory. The operator \mathcal{O}_{3q} vanishes by the fermionic equation of motion and it will not contribute to physical observables. So, the last term in Eq. (1) might be omitted, once the coefficients C_1^0, C_{2q}^0 are determined. For an easier comparison with results already available in the literature, we stick to the normalization of the operators as stated above. The coefficients C_1 and C_{2q} of the physical operators can be related with the definitions used in Ref. [11], via the redefinitions $C_1 = c_g (\pi\alpha_s v^2)/\Lambda^2$ and $C_{2q} = 1 + c_q (16\pi\alpha_s v^2)/\Lambda^2$, where Λ denotes the scale of new physics. For intermediate scales Λ the effects of new physics are embedded in the coefficients of the operators of dimension n , with $n \geq 4$. In the decoupling limit ($\Lambda \rightarrow \infty$) (that we assume here) $C_1 \rightarrow 0$ and $C_{2q} \rightarrow 1$ and the higher-dimensional operators decouple. In the next section we will verify through an explicit calculation that these relations hold at one and two loops in the top sector.

Furthermore, one has to perform a redefinition of the parameters and fields present in the EFT. In mass independent renormalization schemes the Appelquist-Carrazone decoupling theorem [13] does not hold and the Green functions usually depend on the heavy masses and mixing parameters present in the full theory. In order to avoid potentially large logarithms and power corrections one has to decouple the heavy particles from the theory [14]. As a consequence, one obtains different Lagrangian parameters in the various energy regimes. They are connected by the so-called decoupling or matching relations. The relations between the quantities defined in the full (MSSM) and effective theories (SMEFT) that are of interest for our study, are given by

$$\begin{aligned}G_{\mu,\nu}^{0,t,a} &= (\zeta_3^{(0)})^{1/2} G_{\mu,\nu}^{0,a}, \\ c^{0,t} &= (\zeta_{3c}^{(0)})^{1/2} c^0, \\ q_L^{0,t} &= (\zeta_{2L}^{(0)})^{1/2} q_L^0, \\ q_R^{0,t} &= (\zeta_{2R}^{(0)})^{1/2} q_L^0, \\ g_s^{0,t} &= \zeta_g^{(0)} g_s^0, \\ m_q^{0,t} &= \zeta_{m_q}^{(0)} m_q^0, \\ h^{0,t} &= (\zeta_h^{(0)})^{1/2} h^0, \\ y_q^{0,t} &= \zeta_{y_q}^{(0)} y_q^0 f_q(\beta),\end{aligned}\tag{3}$$

where $g_s = \sqrt{4\pi\alpha_s}$ is the strong coupling, $y_q = \sqrt{4\pi\alpha_q}$ is the Yukawa coupling, with

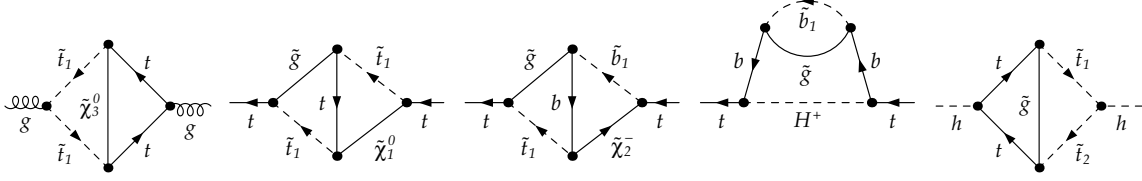


Figure 1: Sample diagrams contributing to ζ_3 , $\zeta_{2L,2R}$, ζ_{m_t} and ζ_h with gluons (g), top quarks (t), and light Higgs (h) as external particles.

$q = b, t$ for the present calculation, and $f_t(\beta) = \sin \beta$ and $f_b(\beta) = \cos \beta$ with $\tan \beta$ defined as the ratio of the vacuum expectation values of the two Higgs doublets. h stands for the field of the lightest neutral Higgs boson. The coefficients $\zeta_3^{(0)}$, $\zeta_{2L}^{(0)}$, $\zeta_{2R}^{(0)}$, $\zeta_g^{(0)}$, $\zeta_m^{(0)}$, $\zeta_h^{(0)}$, $\zeta_{y_q}^{(0)}$ are the bare decoupling coefficients. They may be computed from the transverse part of the gluon polarization function, the vector, axial-vector and scalar part of the quark self-energy, and the Higgs self-energy via [15]

$$\begin{aligned}
\zeta_3^{(0)} &= 1 + \Pi_g^{0,h}(0), \\
\zeta_{2L}^{(0)} &= 1 + \Sigma_v^{0,h}(0) - \Sigma_A^{0,h}(0), \\
\zeta_{2R}^{(0)} &= 1 + \Sigma_v^{0,h}(0) + \Sigma_A^{0,h}(0), \\
\zeta_h^{(0)} &= 1 + \Pi_h^{0,h}(0), \\
\zeta_{m_q}^{(0)} &= \frac{1 - \Sigma_s^{0,h}(0)}{\sqrt{(1 + \Sigma_v^{0,h}(0))^2 - \Sigma_A^{0,h}(0)^2}}.
\end{aligned} \tag{4}$$

The pseudo-scalar part of the quark self-energy vanishes both in the SM and the MSSM through two loops, that renders the equation for $\zeta_m^{(0)}$ in the reduced form given above. Decoupling coefficients are renormalized in a similar manner with the associated parameters and fields [15]. The superscript h indicates that at least one heavy particle is present in the diagrams. Sample Feynman diagrams are shown in Fig. 1.

For the derivation of the coefficient $\zeta_g^{(0)}$ and $\zeta_{y_q}^{(0)}$ one has to consider in addition vertices involving the strong and Yukawa couplings. For example, we chose,

$$\begin{aligned}
\zeta_g^{(0)} &= \frac{\zeta_{gcc}^{(0)}}{\sqrt{\zeta_3^{(0)} \zeta_{3c}^{(0)}}}, \quad \text{with} \quad \zeta_{gcc}^{(0)} = 1 + \Gamma_{gcc}^{0,h}(0,0) \\
\zeta_{y_q}^{(0)} &= \frac{\zeta_{hqq}^{(0)}}{\sqrt{\zeta_h^{(0)} \zeta_{2L}^{(0)} \zeta_{2R}^{(0)}}}, \quad \text{with} \quad \zeta_{hqq}^{(0)} = 1 + \Gamma_{hqq}^{0,h}(0,0).
\end{aligned} \tag{5}$$

Here $\Gamma_{gcc}^{0,h}(0,0)$ and $\Gamma_{hqq}^{0,h}(0,0)$ denote the one-particle-irreducible vertex functions with vanishing momenta flowing through the external legs. Sample Feynman diagrams for the two vertices can be seen in Fig. 2. The decoupling coefficients are independent of the momentum transfer, so that they can be evaluated at vanishing external momenta.

The two-loop SUSY-QCD contributions to ζ_g and ζ_{m_b} for non-vanishing top-quark mass were computed in [16]. The SUSY-QCD contributions for ζ_g , ζ_{m_t} and ζ_{y_t} in the same limit as in the present paper are available from Ref [17]. In addition, two-loop Yukawa contributions to ζ_{m_b} and ζ_{m_τ} were computed in the limit of heavy Higgses (including the lightest one) in Ref. [18]. Two-loop SUSY-QCD and dominant Yukawa contributions for the scalar part of the bottom-quark self energy for the case of an intermediate Higgs mass range (*i.e.* the EFT is the 2HDM) are available from Ref. [19]. The two-loop SUSY-QCD corrections to the vertex functions in the above mentioned limit can be found in Ref. [20]. $\mathcal{O}(\alpha_s\alpha_t)$ corrections to the decoupling coefficients ζ_g , ζ_{m_t} and ζ_{y_t} for a specific mass hierarchy have been computed in [21].

In the present paper we consider the following tree level mass hierarchies

$$\begin{aligned} M_{\text{SUSY}}; M_{\tilde{Q}}; M_{\tilde{D}}; M_{\tilde{U}}; M_{\tilde{g}}; \mu &\gg M_t; M_Z \\ M_{\text{SUSY}}; M_H \simeq M_{H^\pm} \simeq M_A &\gg M_Z; M_h, \end{aligned} \quad (6)$$

where the semicolon between the mass parameters indicates that they are of similar size but not necessarily equal and \simeq means that the masses are equal up to corrections of $\mathcal{O}(M_Z^2/M_A^2)$, that we neglect in the calculation. We introduce M_{SUSY} as a generic heavy mass scale of the order of the supersymmetric particle masses, that will be used in the following discussions. Precisely, for a degenerate supersymmetric mass spectrum it becomes equal to this mass. For a non degenerate spectrum it denotes the mass scale at which the supersymmetric particles become active. The rest of the parameters in the above inequalities denotes the usual soft SUSY breaking parameters in the squark sector. Beyond tree level, it has been shown [22] that this mass hierarchy is stable under radiative corrections. A similar observation holds also for the strongly interacting sector. Let us mention that by expanding in inverse powers of M_A , we get the following relations for the mixing angles in the Higgs sector

$$\begin{aligned} \frac{\cos \alpha}{\sin \beta} &= 1 + \mathcal{O}\left(\frac{M_Z^2}{M_A^2}\right), & -\frac{\sin \alpha}{\cos \beta} &= 1 + \mathcal{O}\left(\frac{M_Z^2}{M_A^2}\right) \\ \sin(\beta - \alpha) &= 1 + \mathcal{O}\left(\frac{M_Z^4}{M_A^4}\right). \end{aligned} \quad (7)$$

These relations parameterize the modifications of the lightest Higgs boson couplings to up-type ($\cos \alpha / \sin \beta$) and down-type ($\sin \alpha / \cos \beta$) quarks and to gauge bosons ($\sin(\beta - \alpha)$) in the MSSM as compared to the SM. Thus, in the decoupling limit the tree-level couplings of the lightest Higgs boson tend to their SM values, as assumed in Eq. (1). These relations hold also at one and two loops and translates into the equality $C_{2t} = 1$ (in the decoupling limit). This will be discussed in more detail below Eq. (16) in the next section.

In the calculation, we take into account the complete one-loop contributions, including genuine electroweak diagrams. At the two-loop order, we neglect electroweak effects (also known as the gaugeless limit). The last approximation is motivated by the small size of the one-loop electroweak effects on the considered parameters. Nevertheless, for the one-loop calculation we assume the following mass hierarchy in the EW sector

$$M_{\text{SUSY}}; M_1; M_2; \mu \gg M_Z; M_W. \quad (8)$$

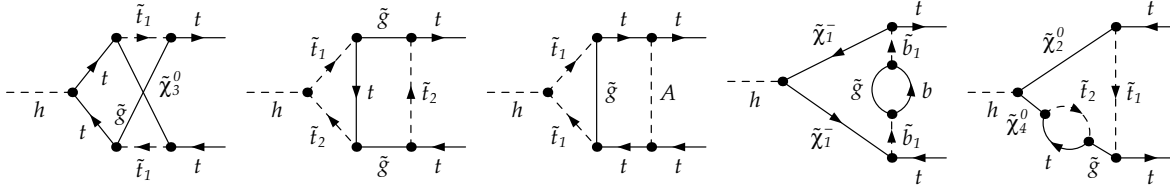


Figure 2: Sample diagrams contributing to ζ_{hqq} .

In this limit, the mass matrices for charginos and neutralinos become diagonal and there is no mixing between higgsinos and electroweakinos. Thus, at the two-loop order we will practically take into account only diagrams with higgsinos.

In our setup, the Feynman diagrams are generated with the program `QGRAF` [23], and further processed with `q2e` and `exp` [24, 25]. In the approximation we worked out, the propagator and vertex topologies can be reduced to two-loop tadpoles [25]. The reduction of various vacuum integrals to the master integral was performed by a self-written `FORM` [26] routine.

For the regularization of the SMEFT we used dimensional regularization (DREG) and for the underlying supersymmetric theory the dimensional reduction (DRED). Technically, we implemented DRED with the help of ε -scalars for the γ, W, Z, g and assigned them heavy masses [16]. There are various ways to perform the explicit calculation. One can in a first step decouple the physical supersymmetric particles using DRED both for the underlying theory as well as for the SMEFT. In a second step, one has to change the regularization scheme from DRED to DREG.² However, in the second step a tower of new ε -scalar couplings, the so called evanescent couplings, have to be taken into account. One can avoid this technical complication using the fact that the change of regularization scheme from DRED to DREG is equivalent to integrating out the ε -scalars from the theory. This last operation means that one can also apply the decoupling procedure to the ε -scalars. Because the physical predictions do not depend on ε -scalar masses, we are free to choose them to be heavy and decouple them together with the heavy supersymmetric particles. In this way, we can perform the change of regularization scheme together with the decoupling procedure. As a consistency check, we verified through two loops that the decoupling coefficients do not depend on the unphysical mass parameters associated with the ε -scalars, as expected. In order to get rid of the unphysical ε -scalar masses, finite shifts in the one-loop renormalization constants for squark masses have to be introduced [28].

For the renormalization of the UV divergences, we employed the minimal subtraction scheme $\overline{\text{DR}}'$ [28] for the coupling constants, quark masses, squark masses and mixing angles and the mass of the ε -scalar associated with the gluon. Explicitly, we keep only the divergent terms in the renormalization constants for all the parameters, except for the squark masses that get finite shifts proportional with the mass of the ε -scalar associated with the gluon. The finite terms are chosen such that the ε -scalar mass M_ε decouples

²For a detailed discussion see for example Ref. [27].

from the system of the renormalization group equations for the squark masses. Explicit formulae for the finite shifts, the renormalization constants for the ε -scalar mass and a detailed description of the method up to three loops in SUSY-QCD can be found in Ref. [29]. The renormalization constants for the parameters $X_t = A_t - \mu/\tan\beta$ and $X_b = A_b - \mu\tan\beta$ can be derived by the chain rule from the definition of the mixing angles. Let us mention that the contributions proportional to the top- and bottom-quark masses in the renormalization constants for the squark masses and mixing angles do not contribute to the decoupling coefficients. However, such terms have to be kept in the derivation of the renormalization constants for X_t and X_b . Explicit one-loop formulae for the renormalization constants for the quark and squark masses and mixing angle can be found in Ref. [18]. For the limit we are interested in here, one has to set the Goldstone boson masses to zero and apply Eqs. (7). Furthermore, we renormalized the tadpole contributions both in the SMEFT and the underlying theory following the prescription introduced in Ref. [30]. It generically requires that

$$\delta t_i^{(l)} + T_i^{(l)} = 0, \quad (9)$$

at all orders in perturbation theory. Here, δt_i denotes the l -loop tadpole counterterm and T_i the l -loop tadpole diagrams, and $i = 1, 2$ sums over the Higgs doublets. In this scheme, no explicit tadpole contributions have to be taken into account in the calculation.

3 Analytical results

The one-loop results for the decoupling coefficients of the gauge and top-Yukawa couplings in the MSSM can be found in Ref. [31]. For completeness we give in the Appendix the one-loop contributions to ζ_{m_t} .

The analytic formulae for the two-loop results are too long to be presented here. They will be used for the numerical analysis in the next section. However, for a better understanding of the numerical effects, we provide below the results for two simplified mass hierarchies. For brevity we display only the contributions of $\mathcal{O}(\alpha_s, \alpha_t, \alpha_s^2, \alpha_s\alpha_t)$. The complete results are submitted in electronic form together with the paper.

A) degenerate mass spectrum:

$$M_{\text{SUSY}} = M_{\tilde{Q}_i} = M_{\tilde{D}_i} = M_{\tilde{U}_i} = M_{\tilde{g}} = M_A = \mu \gg m_t; M_Z; M_h$$

$$\begin{aligned} \zeta_{\alpha_s} = & 1 + a_s \left[C_A \left(-\frac{1}{3} - \frac{2}{3}L_S \right) - \frac{4}{3}I_{2R}n_g L_S \right] + a_s^2 \left[C_A^2 \left(-\frac{5}{18} - \frac{8}{9}L_S + \frac{4}{9}L_S^2 \right) \right. \\ & \left. + C_R I_{2R} n_g \left(\frac{26}{3} - \frac{8}{3}L_S \right) + C_A I_{2R} n_g \left(-\frac{4}{9} + \frac{8}{9}L_S + \frac{16}{9}L_S^2 \right) + \frac{16}{9}I_{2R}^2 n_g^2 L_S^2 \right] \\ & + a_s a_t I_{2R} \left\{ s_\beta^2 \left[\frac{1}{3} - \frac{8}{3}L_S + \left(\frac{10}{9} - 8S_2 \right) \tilde{X}_t^2 \right] + \frac{c_\beta}{s_\beta} \left(-\frac{32}{9} - \frac{8}{3}L_S + 16S_2 \right) \tilde{X}_t \right. \\ & \left. + \frac{1}{s_\beta^2} \left(-\frac{16}{9} - \frac{4}{3}L_S + 8S_2 \right) + \left[-\frac{4}{3} + \frac{20}{3}L_S + \left(-\frac{16}{9} - \frac{4}{3}L_S + 8S_2 \right) \tilde{X}_t^2 \right] \right\}, \quad (10) \end{aligned}$$

$$\begin{aligned}
\zeta_{\alpha t} = & 1 + a_s C_R \left(2 - 2L_S - 2\tilde{X}_t \right) + a_t \left[-\frac{3}{2}L_S - c_\beta^2 \left(\frac{3}{4} + \frac{3}{2}L_S \right) - \frac{1}{2}s_\beta^2 \tilde{X}_t^2 \right] \\
& + a_s^2 \left\{ C_R^2 \left[\frac{119}{12} - \frac{5}{3}L_S + 2L_S^2 + \left(-\frac{4}{3} + \frac{28}{3}L_S \right) \tilde{X}_t + \tilde{X}_t^2 \right] \right. \\
& + C_A C_R \left[\frac{217}{36} - \frac{25}{3}L_S - L_S^2 + \left(-\frac{16}{3} - 8L_S \right) \tilde{X}_t \right] \\
& + C_R I_{2R} n_g \left[\frac{170}{9} - 16L_S + 8L_S^2 + \left(-\frac{16}{3} + \frac{32}{3}L_S \right) \tilde{X}_t \right] \left. \right\} \\
& + a_s a_t C_R \left\{ s_\beta^2 \left[-\frac{67}{4} + \frac{61}{2}L_S - \frac{9}{2}L_S^2 + \frac{459}{4}S_2 + 9\zeta(2) + \left(\frac{11}{2} - 6L_S + \frac{27}{2}S_2 \right) \tilde{X}_t \right. \right. \\
& + \left(-\frac{67}{12} + L_S - 3S_2 \right) \tilde{X}_t^2 + \left(\frac{8}{3} - 12S_2 \right) \tilde{X}_t^3 \left. \right] + \frac{c_\beta}{s_\beta} \left[6 + 6L_S - \frac{27}{2}S_2 \right. \\
& + \left(-\frac{13}{3} - 4L_S + 15S_2 \right) \tilde{X}_t + \left(-\frac{16}{3} - 4L_S + 24S_2 \right) \tilde{X}_t^2 \left. \right] + \frac{1}{s_\beta^2} \left[-\frac{13}{6} - 2L_S \right. \\
& + 12S_2 + \left(-\frac{8}{3} - 2L_S + 12S_2 \right) \tilde{X}_t \left. \right] + \left[-\frac{9}{4} - \frac{11}{2}L_S - \frac{459}{4}S_2 - 9\zeta(2) \right. \\
& + \left(\frac{23}{2} + 16L_S - \frac{27}{2}S_2 \right) \tilde{X}_t + \left(-\frac{13}{6} - 2L_S + 3S_2 \right) \tilde{X}_t^2 \\
& \left. \left. + \left(-\frac{8}{3} - 2L_S + 12S_2 \right) \tilde{X}_t^3 \right] \right\}, \tag{11}
\end{aligned}$$

$$\begin{aligned}
\zeta_{m_t} = & 1 + a_s C_R \left(1 - L_S - \tilde{X}_t \right) + a_t \left[s_\beta^2 \left(\frac{3}{8} + \frac{3}{4}L_S \right) - \left(\frac{3}{8} + \frac{3}{2}L_S \right) \right] \\
& + a_s^2 \left\{ C_R^2 \left[\frac{107}{24} + \frac{1}{6}L_S + \frac{1}{2}L_S^2 + \left(\frac{1}{3} + \frac{11}{3}L_S \right) \tilde{X}_t \right] \right. \\
& + C_A C_R \left[\left(\frac{217}{72} - \frac{25}{6}L_S - \frac{1}{2}L_S^2 \right) + \left(-\frac{8}{3} - 4L_S \right) \tilde{X}_t \right] \\
& + C_R I_{2R} n_g \left[\left(\frac{85}{9} - 8L_S + 4L_S^2 \right) + \left(-\frac{8}{3} + \frac{16}{3}L_S \right) \tilde{X}_t \right] \left. \right\} \\
& + a_s a_t C_R \left\{ s_\beta^2 \left[-\frac{37}{8} + \frac{83}{8}L_S + \frac{459S_2}{8} + \frac{9\zeta(2)}{2} + \left(-\frac{7}{8} - \frac{5}{4}L_S + \frac{27}{4}S_2 \right) \tilde{X}_t \right. \right. \\
& - \left(\frac{13}{24} + \frac{3}{2}S_2 \right) \tilde{X}_t^2 + \left(\frac{5}{6} - 6S_2 \right) \tilde{X}_t^3 \left. \right] + \frac{c_\beta}{s_\beta} \left[3 + 3L_S - \frac{27}{4}S_2 \right. \\
& \left. + \left(-\frac{13}{6} - 2L_S + \frac{15}{2}S_2 \right) \tilde{X}_t + \left(-\frac{8}{3} - 2L_S + 12S_2 \right) \tilde{X}_t^2 \right]
\end{aligned}$$

$$\begin{aligned}
& + \frac{1}{s_\beta^2} \left[\left(-\frac{13}{12} - L_S + 6S_2 \right) - \left(\frac{4}{3} + L_S - 6S_2 \right) \tilde{X}_t \right] \\
& + \left[-\frac{3}{4} - \frac{13}{8} L_S - \frac{3}{2} L_S^2 - \frac{459S_2}{8} - \frac{9\zeta(2)}{2} + \left(\frac{43}{8} + \frac{13}{2} L_S - \frac{27}{4} S_2 \right) \tilde{X}_t \right. \\
& \left. + \left(-\frac{13}{12} - L_S + \frac{3}{2} S_2 \right) \tilde{X}_t^2 + \left(-\frac{4}{3} + 6S_2 - L_S \right) \tilde{X}_t^3 \right] \Big\}, \tag{12}
\end{aligned}$$

where $a_i = \alpha_i/(4\pi)$, $S_2 = \frac{4}{9\sqrt{3}}\text{Cl}_2(\frac{\pi}{3}) \simeq 0.260434$ and $\zeta(2) = \frac{\pi^2}{6}$. C_A, C_R are the $SU(3)$ Casimir invariants for the adjoint and fundamental representations, $I_{2R} = 1/2$, and $n_g = 3$ denotes the number of generations. We have used further the abbreviations $\tilde{X}_t = \frac{X_t}{M_{\text{SUSY}}}$, $L_S = \ln\left(\frac{\mu_{\text{dec}}^2}{M_{\text{SUSY}}^2}\right)$, $c_\beta = \cos\beta$ and $s_\beta = \sin\beta$, where μ_{dec} denotes the decoupling scale at which the heavy degrees of freedom are integrated out. Its precise value is not fixed by theory. Since the explicit dependence on this matching scale is logarithmic, it is natural to choose $\mu_{\text{dec}} \approx M_{\text{SUSY}}$. The dependence of theoretical predictions on the variation of the matching scale around this intuitive value can be used as an estimate of the theoretical uncertainty. Reduction of this uncertainty can only be achieved by means of higher order calculations.

B) light higgsino masses:

$$M_{\text{SUSY}} = M_{\tilde{Q}_i} = M_{\tilde{D}_i} = M_{\tilde{U}_i} = M_{\tilde{g}} = M_A \gg \mu \gg m_t; M_Z; M_h$$

$$\begin{aligned}
\zeta_{\alpha_s} = & 1 + a_s \left[C_A \left(-\frac{1}{3} - \frac{2}{3} L_S \right) - \frac{4}{3} I_{2R} n_g L_S \right] + a_s^2 \left[C_A^2 \left(-\frac{5}{18} - \frac{8}{9} L_S + \frac{4}{9} L_S^2 \right) \right. \\
& \left. + C_R I_{2R} n_g \left(\frac{26}{3} - \frac{8}{3} L_S \right) + C_A I_{2R} n_g \left(-\frac{4}{9} + \frac{8}{9} L_S + \frac{16}{9} L_S^2 \right) + \frac{16}{9} I_{2R}^2 n_g^2 L_S^2 \right] \\
& + a_s a_t I_{2R} \left\{ s_\beta^2 \left[\frac{1}{3} - \frac{8}{3} L_S + \left(\frac{10}{9} - 8S_2 \right) \tilde{X}_t^2 \right] + \frac{c_\beta}{s_\beta} \left(-\frac{32}{9} - \frac{8}{3} L_S + 16S_2 \right) \tilde{X}_t \frac{\mu}{M_S} \right. \\
& + \frac{1}{s_\beta^2} \left(-\frac{16}{9} - \frac{4}{3} L_S + 8S_2 \right) \frac{\mu^2}{M_S^2} + \left[-\frac{4}{3} + 4L_S + \frac{8}{3} (1 + L_S) \frac{\mu^2}{M_S^2} \right. \\
& \left. \left. + \frac{8}{3} L_{\mu M_S} \frac{\mu^4}{M_S^4} + \left(-\frac{16}{9} - \frac{4}{3} L_S + 8S_2 \right) \tilde{X}_t^2 \right] \right\} + \mathcal{O}\left(\frac{\mu^6}{M_S^6}\right), \tag{13}
\end{aligned}$$

$$\begin{aligned}
\zeta_{\alpha_t} = & 1 + a_s C_R \left(2 - 2L_S - 2\tilde{X}_t \right) + a_t \left[-\frac{3}{4} - \frac{3}{2} L_S + \frac{3}{2} \frac{\mu^2}{M_S^2} + \frac{3}{2} (1 + L_{\mu M_S}) \frac{\mu^4}{M_S^4} \right. \\
& - c_\beta^2 \left(\frac{3}{4} + \frac{3}{2} L_S \right) - \frac{1}{2} s_\beta^2 \tilde{X}_t^2 \Big] + a_s^2 \left\{ C_R^2 \left[\frac{119}{12} - \frac{5}{3} L_S + 2L_S^2 + \left(-\frac{4}{3} + \frac{28}{3} L_S \right) \tilde{X}_t \right. \right. \\
& \left. \left. + \tilde{X}_t^2 \right] + C_A C_R \left[\frac{217}{36} - \frac{25}{3} L_S - L_S^2 + \left(-\frac{16}{3} - 8L_S \right) \tilde{X}_t \right] \right. \\
& \left. + C_R I_{2R} n_g \left[\frac{170}{9} - 16L_S + 8L_S^2 + \left(-\frac{16}{3} + \frac{32}{3} L_S \right) \tilde{X}_t \right] \right\}
\end{aligned}$$

$$\begin{aligned}
& + a_s a_t C_R \left\{ s_\beta^2 \left[-\frac{67}{4} + \frac{61}{2} L_S - \frac{9}{2} L_S^2 + \frac{459}{4} S_2 + 9\zeta(2) + \left(\frac{11}{2} - 6L_S + \frac{27}{2} S_2 \right) \tilde{X}_t \right. \right. \\
& + \left(-\frac{67}{12} + L_S - 3S_2 \right) \tilde{X}_t^2 + \left(\frac{8}{3} - 12S_2 \right) \tilde{X}_t^3 \left. \right] + \frac{c_\beta}{s_\beta} \left[6 + 6L_S - \frac{27}{2} S_2 \right. \\
& + \left(-\frac{13}{3} - 4L_S + 15S_2 \right) \tilde{X}_t + \left(-\frac{16}{3} - 4L_S + 24S_2 \right) \tilde{X}_t^2 \left. \right] \frac{\mu}{M_S} \\
& + \frac{1}{s_\beta^2} \left[-\frac{13}{6} - 2L_S + 12S_2 + \left(-\frac{8}{3} - 2L_S + 12S_2 \right) \tilde{X}_t \right] \frac{\mu^2}{M_S^2} \\
& + \left[-\frac{37}{2} - 9L_S - \frac{459}{4} S_2 + \frac{3}{2} \zeta(2) + \left(-\frac{49}{2} + L_S + 15\zeta(2) \right) \frac{\mu^2}{M_S^2} \right. \\
& + \left(-\frac{477}{8} - \frac{89}{4} L_S - 9L_S^2 + \frac{29}{4} L_\mu + 9L_S L_\mu + 24\zeta(2) \right) \frac{\mu^4}{M_S^4} \\
& + \left[1 + 12L_S - \frac{27}{2} S_2 + 6\zeta(2) + (-5 + 4L_S + 6\zeta(2)) \frac{\mu^2}{M_S^2} \right. \\
& + \left(-\frac{21}{2} + 4L_\mu M_S + 6\zeta(2) \right) \frac{\mu^4}{M_S^4} \left. \right] \tilde{X}_t + \left(-\frac{13}{6} - 2L_S + 3S_2 \right) \tilde{X}_t^2 \\
& + \left. \left(-\frac{8}{3} - 2L_S + 12S_2 \right) \tilde{X}_t^3 \right\} + \mathcal{O} \left(\frac{\mu^6}{M_S^6} \right), \tag{14}
\end{aligned}$$

$$\begin{aligned}
\zeta_{m_t} = & 1 + a_s C_R \left(1 - L_S - \tilde{X}_t \right) + a_t \left[s_\beta^2 \left(\frac{3}{8} + \frac{3}{4} L_S \right) - \frac{3}{4} - \frac{3}{2} L_S + \frac{3}{4} \frac{\mu^2}{M_S^2} \right. \\
& + \left. \frac{3}{4} (1 + L_\mu M_S) \frac{\mu^4}{M_S^4} \right] + a_s^2 \left\{ C_R^2 \left[\frac{107}{24} + \frac{1}{6} L_S + \frac{1}{2} L_S^2 + \left(\frac{1}{3} + \frac{11}{3} L_S \right) \tilde{X}_t \right] \right. \\
& + C_A C_R \left[\left(\frac{217}{72} - \frac{25}{6} L_S - \frac{1}{2} L_S^2 \right) + \left(-\frac{8}{3} - 4L_S \right) \tilde{X}_t \right] \\
& + \left. C_R I_{2R} n_g \left[\left(\frac{85}{9} - 8L_S + 4L_S^2 \right) + \left(-\frac{8}{3} + \frac{16}{3} L_S \right) \tilde{X}_t \right] \right\} \\
& + a_s a_t C_R \left\{ s_\beta^2 \left[-\frac{37}{8} + \frac{83}{8} L_S + \frac{459 S_2}{8} + \frac{9\zeta(2)}{2} + \left(-\frac{7}{8} - \frac{5}{4} L_S + \frac{27}{4} S_2 \right) \tilde{X}_t \right. \right. \\
& - \left(\frac{13}{24} + \frac{3}{2} S_2 \right) \tilde{X}_t^2 + \left(\frac{5}{6} - 6S_2 \right) \tilde{X}_t^3 \left. \right] + \frac{c_\beta}{s_\beta} \left[3 + 3L_S - \frac{27}{4} S_2 \right. \\
& + \left. \left(-\frac{13}{6} - 2L_S + \frac{15}{2} S_2 \right) \tilde{X}_t + \left(-\frac{8}{3} - 2L_S + 12S_2 \right) \tilde{X}_t^2 \right] \frac{\mu}{M_S}
\end{aligned}$$

$$\begin{aligned}
& + \frac{1}{s_\beta^2} \left[\left(-\frac{13}{12} - L_S + 6S_2 \right) - \left(\frac{4}{3} + L_S - 6S_2 \right) \tilde{X}_t \right] \frac{\mu^2}{M_S^2} \\
& + \left[-\frac{17}{2} - \frac{15}{4}L_S - \frac{3}{2}L_S^2 - \frac{459S_2}{8} + \frac{3}{4}\zeta(2) + \left(-13 + \frac{5}{4}L_S + \frac{15}{2}\zeta(2) \right) \frac{\mu^2}{M_S^2} \right. \\
& + \left(-\frac{489}{16} - \frac{89}{8}L_S - \frac{15}{4}L_S^2 + \frac{35}{8}L_\mu + \frac{15}{4}L_S L_\mu + 12\zeta(2) \right) \frac{\mu^4}{M_S^4} \\
& \left. \left[-\frac{1}{4} + \frac{9}{2}L_S - \frac{27}{4}S_2 + 3\zeta(2) + \left(-\frac{7}{4} + 2L_S + 3\zeta(2) \right) \frac{\mu^2}{M_S^2} \right. \right. \\
& + \left. \left(-\frac{9}{2} + \frac{11}{4}L_{\mu M_S} + 3\zeta(2) \right) \frac{\mu^4}{M_S^4} \right] \tilde{X}_t + \left(-\frac{13}{12} - L_S + \frac{3}{2}S_2 \right) \tilde{X}_t^2 \\
& + \left. \left(-\frac{4}{3} + 6S_2 - L_S \right) \tilde{X}_t^3 \right] \} + \mathcal{O} \left(\frac{\mu^6}{M_S^6} \right), \tag{15}
\end{aligned}$$

where $L_{\mu M_S} = \ln \left(\frac{\mu^2}{M_{\text{SUSY}}^2} \right)$ and a_s and a_t denote the MSSM couplings.

For the derivation of the above formulae we implemented two methods. In one approach, we expanded the two-loop analytical results for a general mass spectrum in the above given mass hierarchies. In the second approach, we asymptotically expanded the Feynman integrals with the code `exp` and afterwards used the one-mass scale tadpole integrals from the code `MATAD` [32]. We found full agreement between the two approaches.

Analytical expressions for the dominant two-loop contributions to $\Sigma_{s,b}$ in the case of a degenerate SUSY spectrum, but for intermediate Higgs masses can be found in [19]. We have computed $\zeta_{s,b}$ also for this mass hierarchy, and after translating our results into the renormalization and regularization schemes used in that reference, we found full analytical agreement.

Another interesting consistency check of our calculation is to show that the Wilson coefficients introduced in Eq. (1) reach their SM values when the decoupling limit is applied. Explicitly, it holds

$$C_i = C_i^{\text{SM}} + \mathcal{O} \left(\frac{m_t^2}{M_{\text{SUSY}}^2}, \frac{M_Z^2}{M_{\text{SUSY}}^2}, \frac{M_h^2}{M_{\text{SUSY}}^2}, \right) \quad \text{with } i = g, 2t, 3t. \tag{16}$$

The mass suppressed terms will give contributions to Wilson coefficients associated with dimension 6 or higher operators [11], that are beyond the scope of the present paper. At the one-loop level, it is an easy exercise to apply the decoupling limit as stated in Eqs. (6) and (7) to the known results from Refs. [19, 20] and get $C_{2t} = 1$, $C_g = 0$ and $C_{3t} = 0$. The first relation is guaranteed by the alignment limit Eq. (7), whereas the other two are due to the limit $m_t \rightarrow 0$. At $\mathcal{O}(\alpha_s^2, \alpha_s \alpha_t, \alpha_s \alpha_b)$ we have explicitly verified that in the decoupling limit $C_{2t} = 1$, that amounts to show that the corrections to vertex function $\Gamma_{htt}^h(0, 0)$ and to the scalar part of the top-quark selfenergy $\Sigma_s^h(0)$ are equal up to a sign. Furthermore, the vertex function $\Gamma_{htt}^h(0, 0)$ does not get vector or axial-vector components, so that C_{3q} remains equal to zero³ and no mixing between \mathcal{O}_{2t} and \mathcal{O}_{3t} occurs at the given order.

³See Ref. [20] for details.

Moreover, we also proved that

$$\zeta_v = \frac{\zeta_{m_t}}{\zeta_{y_t}}, \quad (17)$$

where ζ_{y_t} and ζ_{m_t} were defined in Eqs. (5) and (4). The decoupling coefficient for the vacuum expectation value ζ_v can be derived from the relation $M_W = g_2 v/2$. At $\mathcal{O}(\alpha_t)$ and $\mathcal{O}(\alpha_s \alpha_t)$ only the transversal part of the W -boson propagator contributes, because the decoupling coefficient of the gauge coupling g_2 receives only corrections of $\mathcal{O}(\alpha_2)$ or higher. Therefore, at this level of accuracy holds

$$\zeta_v = 1 + \frac{\Pi_W^{T,h}(0)}{2M_W^2}. \quad (18)$$

As can be understood from the analytical expression displayed above, the decoupling coefficients for α_s , α_t and m_t have a remnant logarithmic dependence on the new physics scale (in our case it is identified with M_{SUSY}) and a polynomial dependence on the mixing parameters even for the case that $M_{\text{SUSY}} \gg M_{\text{EW}}$. These corrections we denote generically as non decoupling effects, in the sense that they do not vanish when the scale of new physics become much heavier than the electroweak one. Therefore, the energy evolution of the three fundamental parameters contain important informations about the underlying theory, even in the challenging case of the decoupling scenario.

4 Numerics

In this section, we study the phenomenological implications of the two-loop calculation presented above. For our analysis we consider the strong coupling constant, the top-quark mass and the top-Yukawa coupling. For a detailed study on the bottom sector we refer for example to Refs. [19, 20]. For the SM input parameters we employed the following numerical values: $M_W = 80.387 \pm 0.016$ GeV, $M_t = 173.34 \pm 0.81$ GeV, $M_h = 125.09 \pm 0.24$ GeV and $\alpha_s(M_Z) = 0.1181 \pm 0.011$ [33]. For the SUSY parameters, we focus on two benchmark scenarios that are still allowed by the direct searches at the LHC. The first scenario is the pMSSM as defined in Ref. [34] and is characterized by a heavy higgsino sector in the TeV range. More precisely, the numerical values of the specific parameters read $\mu = 2.5$ TeV, $A_t = -4.8$ TeV, $\tan \beta = 10$, $M_A = 1.5$ TeV, $M_{\tilde{g}} = 1$ TeV, $M_Q \simeq M_U \simeq M_D \simeq 2.5$ TeV. The second scenario we study is a MSUGRA based scenario as introduced in Ref. [35], with heavy SUSY particles up to 6 TeV but light electroweakino around 200 GeV. Explicitly, $m_0 = 6183$ GeV, $m_{1/2} = 470$ GeV, $A_0 = -4469$ GeV, $\tan \beta = 10$, $\mu > 0$.

Two-loop decoupling effects are usually combined with three-loop renormalization group equations (RGEs) in order to properly resum the logarithms that arise in the calculation. For a detailed discussion of the running and decoupling procedure within the $\overline{\text{MS}}$ scheme we refer to Ref. [36]. The application of the method to the $\overline{\text{DR}}$ scheme follows in complete analogy.

For the current analysis, we implement the three-loop RGEs for the gauge and Yukawa couplings from Refs. [37] for the SM and from Ref. [38] for the MSSM. The three-loop anomalous dimension for the top-quark mass is not available in the literature neither in the SM nor in the MSSM. However, the genuine QCD and SUSY-QCD contributions can be derived from the beta-function of the top-Yukawa coupling. The dominant mixed (SUSY)QCD-Yukawa contributions of $\mathcal{O}(\alpha_s^2\alpha_t, \alpha_s\alpha_t^2)$ we have computed explicitly and implemented in our numerical analysis. Furthermore, we took into account the electroweak contributions at two loops in the running and at one loop in the decoupling coefficients. As it is well known, when the tadpole contributions are renormalized to zero, there is a gauge dependence of the running masses. In our setup, we chose the Feynman-gauge for the electroweak sector. Nevertheless, the decoupling coefficients for the running masses remain gauge independent. In our numerical analysis, the gauge dependence is hidden in the SM value of $m_t(M_t)$ that is our starting value for the running analysis.

The choice of the scale μ_{dec} at which the SM is matched with the MSSM is not fixed by the theory and any remnant dependence of the physical parameters on it is a measure of the theoretical uncertainties. In Fig. 3 we show the dependence on this scale for $m_t(\mu_{\text{ren}} = 200 \text{ GeV})$, $\alpha_t(\mu_{\text{ren}} = 200 \text{ GeV})$, and $\alpha_s(\mu_{\text{ren}} = 1 \text{ TeV})$ within the pMSSM scenario. The dotted (blue), dashed (red) and full (black) lines in the figure correspond to one-, two- and three-loop running. The dot-dashed lines stand for the three-loop SUSY-QCD contributions. Explicitly, to obtain this plot we employed the three-loop RGEs for QCD and SUSY-QCD and the $\mathcal{O}(\alpha_s, \alpha_s^2)$ contributions to the decoupling coefficients. As expected, going from one- to two- and three-loop order the matching scale dependence stabilizes and the three-loop results are practically independent. It is also interesting to observe that the matching scale dependence at two loops exceeds the current experimental uncertainty on m_t and α_s by about a factor of two.

Furthermore, the best choice for the matching scale (defined as the scale where the higher order radiative corrections are minimal) is different for m_t , α_t and α_s , respectively. This feature can be understood from Eqs. (10,11,12) and (13,14,15). For α_s the best choice of μ_{dec} is approximately given by the average mass of the coloured SUSY particles. In the top sector, however, the logarithmic dependence on the mass parameters is supplemented by the terms proportional with $\tilde{X}_t, \tilde{X}_t^2, \tilde{X}_t^3$. For the pMSSM scenario $\tilde{X}_t \simeq 2$ and the scale at which the radiative corrections vanish increases towards 6 TeV. For small X_t values, *e.g.* for small trilinear coupling A_t and large values for $\tan\beta$, the terms proportional with powers of \tilde{X}_t will drop off and ζ_{m_t} and ζ_{y_t} will have almost a logarithmic dependence on the masses of the supersymmetric particles.

In principle, one can perform the decoupling procedure at each mass threshold. This approach guarantees the absence of potentially large logarithmic and power corrections. However, a tower of intermediate non supersymmetric effective theories with a complicated mixing pattern will arise. In our framework we avoid these computational complications by decoupling all heavy particles in one step. Nevertheless, in order to reduce the dependence of the theoretical predictions on the matching scale, we have to take into account higher order radiative corrections. Fig. 3 demonstrates the necessity for the two loop corrections to the decoupling coefficients and their phenomenological implications.

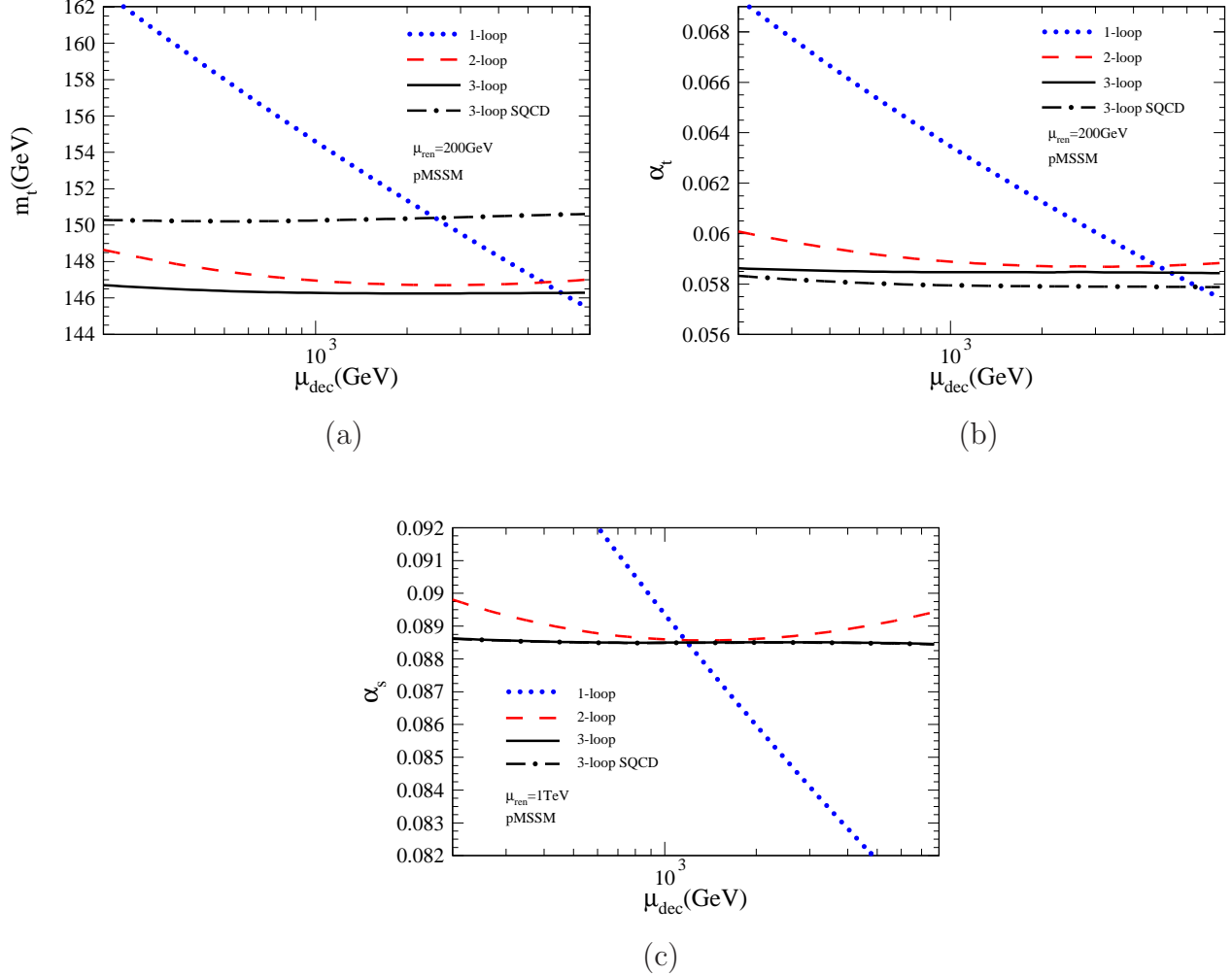


Figure 3: $m_t(\mu_{\text{ren}} = 200 \text{ GeV})$, $\alpha_t(\mu_{\text{ren}} = 200 \text{ GeV})$, and $\alpha_s(\mu_{\text{ren}} = 1 \text{ TeV})$ as functions of μ_{dec} . The dotted, dashed and full lines correspond to one-, two- and three-loop running. The dot-dashed lines display the three-loop SUSY-QCD contributions.

The top-Yukawa contributions are of phenomenological relevance only for m_t and α_t , as can be read from the difference between the full and dot-dashed lines in Fig. 3. For example, the top-Yukawa contributions to $m_t(\mu_{\text{ren}} = 200 \text{ GeV})$ amounts to about 4 GeV, a value almost four times larger than the same quantity within the SM. The 4 GeV in the running mass in the MSSM can be explained through the top-Yukawa effects both on the running and on the decoupling. This aspect is also nicely illustrated in Fig. 5(a), where for the chosen decoupling scale of $\mu_{\text{dec}} = 400 \text{ GeV}$ the dominant effects are induced by the modifications in the RGEs due to Yukawa couplings. It is also interesting to note

that the relative size between SUSY-QCD and top-Yukawa contributions varies with the choice of the renormalization scale, as can be understood from Fig. 4. For the α_s , however, the top-Yukawa contributions are not phenomenologically relevant, as can be understood from the superposition of the dot-dashed and full lines in the lower plot of Fig. 3.

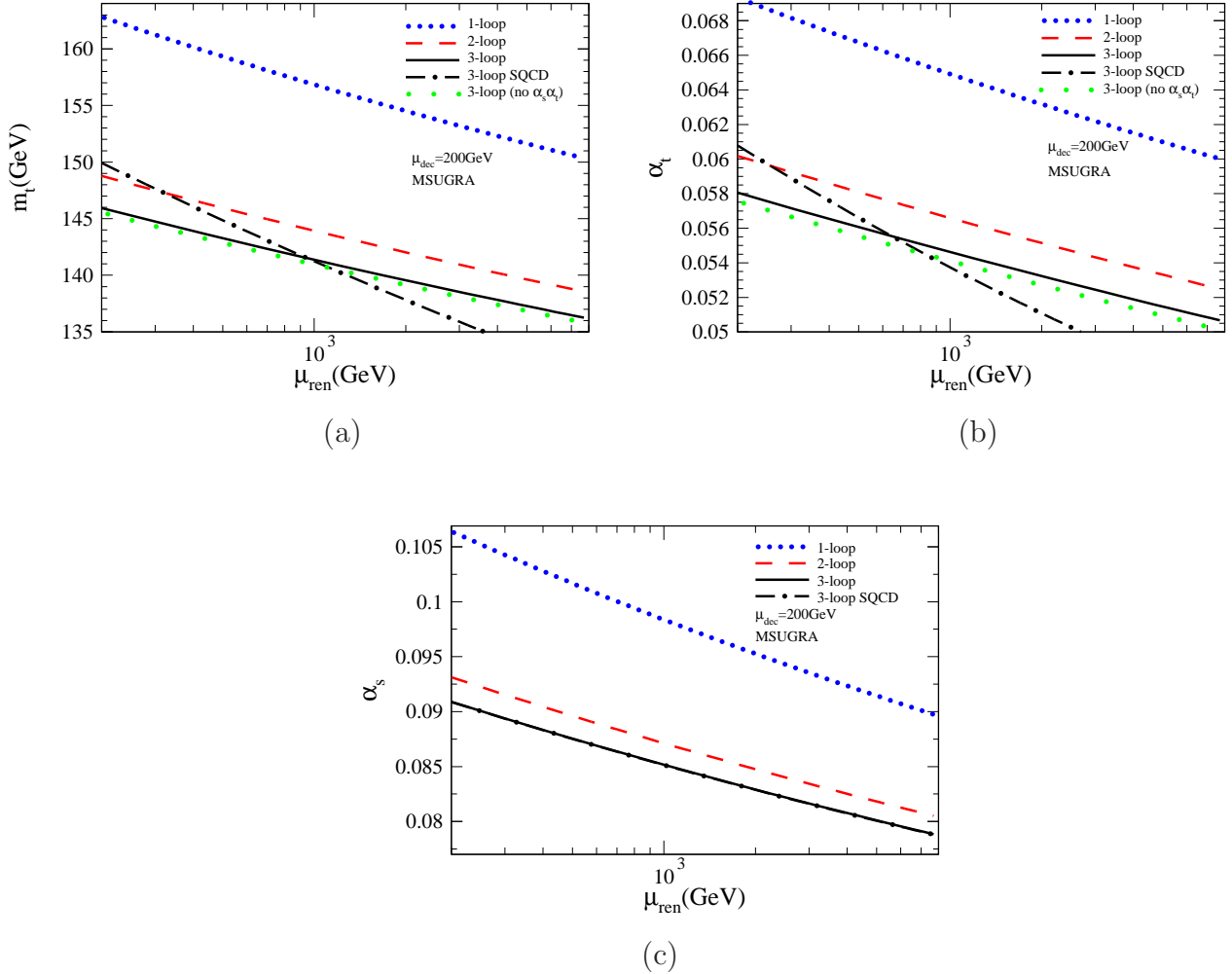


Figure 4: Renormalization scale dependence for m_t , α_t , and α_s for $\mu_{\text{dec}} = 200 \text{ GeV}$. The dotted, dashed and full lines correspond to one-, two- and three-loop running. The dot-dashed lines display the three-loop SUSY-QCD contributions. The large dotted lines marked in the legend with the label (no $\alpha_s \alpha_t$) show the predictions of the three-loop analysis, where the $\mathcal{O}(\alpha_s \alpha_t)$ contributions to the decoupling coefficients for m_t and α_t were excluded.

In Fig. 4 the renormalization scale dependence of m_t , α_t and α_s within the MSUGRA scenario is shown, where the matching scale was fixed at $\mu_{\text{dec}} = 200 \text{ GeV}$. The convention

for the lines is the same as in the previous figure up to the large dotted lines that display the three-loop analysis, for which the $\mathcal{O}(\alpha_s\alpha_t)$ contributions to the decoupling coefficients were not taken into account. Let us mention that the size of the three-loop contributions is few times larger than the current experimental uncertainties for m_t and α_s [33] and comparable with the expected accuracy on α_t at future colliders. As can be understood from comparing the full and dot-dashed lines in the figure, the genuine SUSY-QCD contributions are sufficient for the prediction of the energy evolution of α_s . However, the running of m_t and α_t receive significant corrections from the Yukawa and/or mixed QCD-Yukawa sectors, that can well exceed the current experimental accuracy at high energy scales. Let us also mention that the $\mathcal{O}(\alpha_t, \alpha_s\alpha_t)$ corrections to the running and threshold effects within the MSSM are few times larger than in the SM. This behaviour can be explained by the interplay between the masses and the mixing parameters of the model. Moreover, as can be understood from the comparison of the solid and large dotted lines, the contributions of $\mathcal{O}(\alpha_s\alpha_t)$ to the decoupling coefficients have a small numerical effect, well below the experimental accuracy.

For a better understanding of the phenomenological implications we show in Fig. 5 the scale evolution of the three parameters both in the SM and the MSSM for the pMSSM scenario, where the matching between the two theories was performed at $\mu_{\text{dec}} = 400$ GeV. Namely, below 400 GeV the SM is considered as the theory describing the physical phenomena. Above this energy scale, the MSSM is the underlying theory. For the dot-dashed lines, only the QCD (below $\mu_{\text{dec}} = 400$ GeV) and SUSY-QCD (above $\mu_{\text{dec}} = 400$ GeV) contributions are taken into account. For the one-loop running (dotted lines in the plots) only a change of slopes occurs, because no decoupling is taken into account. At two and three loops, the running is accompanied by one- and two-loop decoupling. The vertical shifts at $\mu_{\text{ren}} = \mu_{\text{dec}} = 400$ GeV display directly the effects of the decoupling procedure. The numerical values of the mixed (SUSY)QCD-Yukawa contributions at three loops can be read from the difference between the full and the dot-dashed curves in the figure. As already pointed out, their magnitude depends on the scale choice and are phenomenologically significant for the top sector of the MSSM. The magnitude of the $\mathcal{O}(\alpha_s\alpha_t)$ corrections to the decoupling coefficients for m_t and α_t can be read from the difference between the solid and the large dotted lines. For the MSSM scenario under consideration, they are much smaller than the expected experimental precision.

5 Conclusions

In this paper we have calculated two loop mixed QCD-Yukawa corrections to the decoupling coefficients for the strong coupling, the top-Yukawa coupling and the top quark mass. As underlying theory we considered the MSSM and decoupled all the supersymmetric particles in one step. The price for this simplifying assumption is the necessity for two-loop corrections to the matching coefficients for the fundamental parameters like coupling constants and particle masses. The two-loop decoupling coefficients together with the three-loop RGEs ensure the independence of the decoupling procedure on the

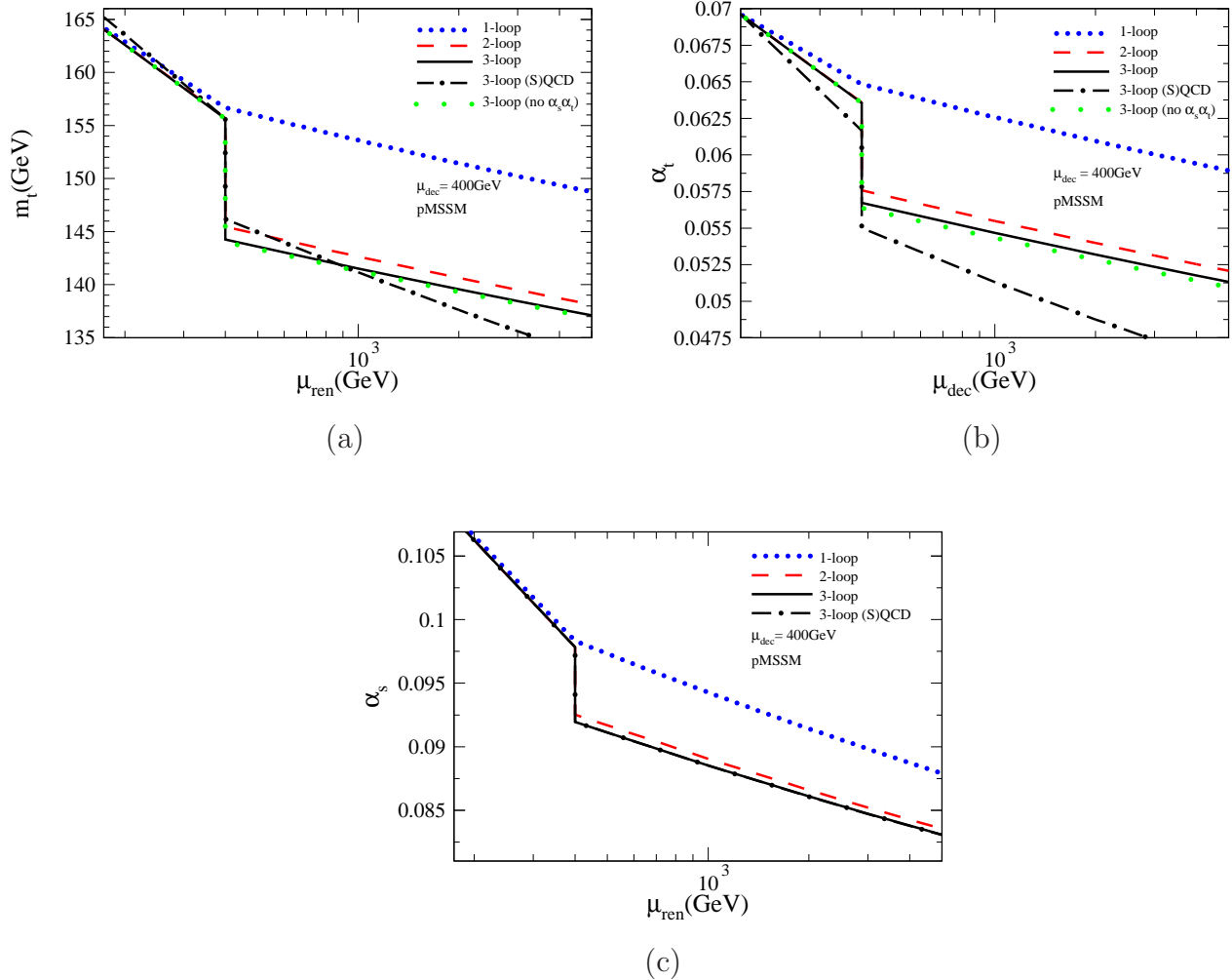


Figure 5: Running of m_t , α_t , and α_s . The matching scale between the SM and the MSSM is $\mu_{\text{dec}} = 400 \text{ GeV}$. The convention for the lines is as in the previous plot. The jumps at $\mu_{\text{dec}} = 400$ display the decoupling effects.

scale at which the heavy particles are integrated out, up to higher order terms in α_s and α_t .

Although the running masses and couplings are themselves not physical observables, they are necessary ingredients for the theoretical predictions of cross sections, branching ratios or physical masses. For example, if in a diagrammatic calculation performed within the MSSM at fixed order or in the EFT approach the running top-quark mass and/or running top-Yukawa and strong couplings are used, then the non-decoupling effects we discussed here are implicitly contained in the numerical values of the running parameters. Depending on the order in perturbation theory at which the calculation is

performed, the $\mathcal{O}(\alpha_s^2, \alpha_s \alpha_t)$ might not be required. In this case the decoupling scale have to be carefully chosen in order to avoid missing large higher order radiative corrections to the running parameters as we have shown in Fig. 3.

There is also another method to determine the numerical values of the running top-quark mass and top-Yukawa coupling. Namely, they can be derived from the measured top, W and Z boson, and Higgs pole masses. However, such a determination will get very large radiative corrections for heavy supersymmetric particle [17]. Fig. 3 and Fig. 5 of Ref. [17] display the explicit comparison of the method based on running and decoupling procedure (similar with that presented in the current paper) and the direct calculation starting from the relation between the pole and the running top quark mass within the SUSY-QCD, using the code TSIL [39]. It turned out that, in order to bring the theoretical uncertainties on the running top quark mass at least in the range of the experimental precision, one needs even the three-loop corrections. Such type of calculations are computationally very involved and not yet available in the literature. For the mixed (SUSY)QCD-Yukawa corrections to these relations, we expect a similar behaviour in the perturbative expansion but being technically even more involved. However, from the numerical analysis we presented in the previous section, one can see that the difference between the two- and the three-loop corrections derived within the running and decoupling approach are significantly smaller. For example the genuine three-loop contributions to the running top-quark mass are of about 1 GeV for appropriately chosen decoupling scales, as can be read from Fig. 5(a). This behaviour can be explained by the fact that the large logarithms of the form $\ln(M_{\text{top}}^2/M_{\text{SUSY}}^2)$ are resummed through the use of the RGEs in the SM and the MSSM. In our setup, we use the relation between the pole and the running masses and couplings only within the SM, so that the occurring logarithms of the form $\ln(M_{\text{top}}^2/M_{\text{EW}}^2)$, where $M_{\text{EW}} = M_Z, M_W$ and M_h , are numerically small.

From our numerical analysis it turned out that the genuine $\mathcal{O}(\alpha_s \alpha_t)$ contributions to the matching coefficients are well below the experimental precision. However, the complete $\mathcal{O}(\alpha_t, \alpha_s \alpha_t)$ corrections (including the RGE and the threshold effects) to the running top quark mass amount to about few GeV and for the top-Yukawa coupling reach the percent range. The $\mathcal{O}(\alpha_s \alpha_t)$ corrections to the decoupling coefficients for m_t , α_s and α_t are necessary, for example, for the prediction of the lightest Higgs boson mass in supersymmetric theories and for the vacuum stability studies in such theories, when going beyond two-loop accuracy. The latter are just two examples of current analyses that play key roles in constraining and/or unrevealing the type and scale of new physics.

Furthermore, we provide compact analytical formulae for the decoupling coefficients for two mass hierarchies: i) a completely degenerate supersymmetric mass spectrum and ii) a quasi degenerate supersymmetric mass spectrum with higgsinos much lighter than the rest of the superpartners. Along with this paper we provide the results in electronic form, that should be useful for other calculations.

Acknowledgments

This work was supported by *Deutsche Forschungsgemeinschaft* (contract MI 1358, Heisenberg program). The authors are grateful to M. Steinhauser for collaboration at an early

stage of the project, for numerous enlightening discussions and for reading the manuscript.

A Appendix A

In this appendix we provide the complete one-loop results for the decoupling coefficient of top-quark mass. It reads

$$\begin{aligned}
\zeta_{m_t} = & 1 + a_s \left\{ C_R x_{\text{DRED}} + C_R \left[\frac{1 - 2x_{\tilde{g}Q_3}^2}{2x_{\tilde{g}Q_3}^2} \mathcal{P}_{\tilde{g}Q_3} - \frac{1}{2} \mathcal{P}_{\tilde{g}U_3} + \left(-\frac{1}{2} \mathcal{P}_{\tilde{g}Q_3}^2 - \frac{1}{2} \mathcal{P}_{\tilde{g}U_3}^2 \right) L_{\tilde{g}} \right. \right. \\
& + \left. \left(-\frac{1}{2} + \frac{1}{2} \mathcal{P}_{\tilde{g}Q_3}^2 \right) L_{Q_3} + \left(-\frac{1}{2} + \frac{1}{2} \mathcal{P}_{\tilde{g}U_3}^2 \right) L_{U_3} + \frac{X_t}{m_{Q_3}} \left[\frac{2}{x_{\tilde{g}Q_3}} \mathcal{P}_{\tilde{g}Q_3} \mathcal{P}_{\tilde{g}U_3} L_{\tilde{g}} \right. \right. \\
& \left. \left. - 2x_{\tilde{g}Q_3} \mathcal{P}_{\tilde{g}Q_3} \mathcal{P}_{Q_3U_3} L_{Q_3} + \mathcal{P}_{\tilde{g}Q_3} \left(-\frac{2}{x_{\tilde{g}Q_3}} \mathcal{P}_{\tilde{g}U_3} + 2x_{\tilde{g}Q_3} \mathcal{P}_{Q_3U_3} \right) L_{U_3} \right] \right] \left. \right\} \\
& + a_2 \left[x_{\text{DRED}} \left(-\frac{3}{8} \right) - \frac{3}{16} - \frac{3}{8} \mathcal{P}_{2Q_3} + L_2 - \frac{3}{8} \mathcal{P}_{2Q_3}^2 + \left(-\frac{3}{8} + \frac{3}{8} \mathcal{P}_{2Q_3}^2 \right) L_{Q_3} \right] \\
& + a_1 \left\{ x_{\text{DRED}} \left(-\frac{1}{72} \right) + \frac{17 - 9x_{1Q_3}^2}{144x_{1Q_3}^2} \mathcal{P}_{1Q_3} - \frac{2}{9} \mathcal{P}_{1U_3} + \left(-\frac{1}{72} \mathcal{P}_{1Q_3}^2 - \frac{2}{9} \mathcal{P}_{1U_3}^2 \right) L_1 \right. \\
& + \left. \left(-\frac{1}{72} + \frac{1}{72} \mathcal{P}_{1Q_3}^2 \right) L_{Q_3} + \left(-\frac{2}{9} + \frac{2}{9} \mathcal{P}_{1U_3}^2 \right) L_{U_3} + \frac{X_t}{m_{Q_3}} \left[\frac{2}{9x_{1Q_3}} \mathcal{P}_{1Q_3} \mathcal{P}_{1U_3} L_1 \right. \right. \\
& \left. \left. - \frac{2x_{1Q_3}}{9} \mathcal{P}_{1Q_3} \mathcal{P}_{Q_3U_3} L_{Q_3} + \mathcal{P}_{1Q_3} \left(-\frac{2}{9x_{1Q_3}} \mathcal{P}_{1U_3} + \frac{2x_{1Q_3}}{9} \mathcal{P}_{Q_3U_3} \right) L_{U_3} \right] \right\} \\
& + a_t \left\{ -\frac{9}{8} + \frac{1}{2} \mathcal{P}_{Q_3\mu} + \frac{1}{4} \mathcal{P}_{U_3\mu} + c_\beta^2 \left(-\frac{3}{8} - \frac{3}{4} L_A \right) + \left(-\mathcal{P}_{Q_3\mu} + \frac{1}{2} \mathcal{P}_{Q_3\mu}^2 \right) L_{Q_3} \right. \\
& + \left. \left(-\frac{1}{2} \mathcal{P}_{U_3\mu} + \frac{1}{4} \mathcal{P}_{U_3\mu}^2 \right) L_{U_3} + \left(-\frac{3}{4} + \mathcal{P}_{Q_3\mu} - \frac{1}{2} \mathcal{P}_{Q_3\mu}^2 + \frac{1}{2} \mathcal{P}_{U_3\mu} - \frac{1}{4} \mathcal{P}_{U_3\mu}^2 \right) L_\mu \right\} \\
& + a_b \left\{ -\frac{1}{2} + \frac{1}{4} \mathcal{P}_{D_3\mu} - \frac{1}{4} L_A + c_\beta^2 \left(-\frac{7}{8} - \frac{3}{4} L_A \right) + \left(-\frac{1}{2} \mathcal{P}_{D_3\mu} + \frac{1}{4} \mathcal{P}_{D_3\mu}^2 \right) L_{D_3} \right. \\
& + \left. \left(-\frac{1}{4} + \frac{1}{2} \mathcal{P}_{D_3\mu} - \frac{1}{4} \mathcal{P}_{D_3\mu}^2 \right) L_\mu + \frac{X_b}{\mu t_\beta} \left[-\mathcal{P}_{D_3\mu} \mathcal{P}_{D_3Q_3} L_{D_3} + \mathcal{P}_{D_3Q_3} \mathcal{P}_{Q_3\mu} L_{Q_3} \right. \right. \\
& \left. \left. + \left(\mathcal{P}_{D_3\mu} \mathcal{P}_{D_3Q_3} - \mathcal{P}_{D_3Q_3} \mathcal{P}_{Q_3\mu} \right) L_\mu \right] \right\}, \tag{19}
\end{aligned}$$

where we have used the following notations

$$L_i = \ln(\mu_{\text{dec}}^2/m_i^2) \quad x_{ij} = \frac{m_i}{m_j},$$

$$\mathcal{P}_{ij} = \frac{m_i^2}{m_i^2 - m_j^2} = \frac{1}{1 - \frac{m_j^2}{m_i^2}} = \frac{1}{1 - x_{ji}^2}.$$

Here $M_{Q_3}, M_{U_3}, M_{D_3}$ are the soft SUSY-breaking parameters of the stop- and sbottom-sector, M_1, M_2 and $M_{\tilde{g}}$ denotes the gaugino masses. Here we adopted the SU(5) normalization for the gauge coupling α_1 . The label x_{DRED} marks the contributions induced by the change from DREG to DRED. The results for ζ_{m_b} and ζ_{y_b} can be derived via the following replacements $t \leftrightarrow b$ and $U_3 \leftrightarrow D_3$.

References

- [1] Atlas Collaboration,
<https://twiki.cern.ch/twiki/bin/view/AtlasPublic/SupersymmetryPublicResults>; CMS Collaboration,
<https://twiki.cern.ch/twiki/bin/view/CMSPublic/PhysicsResultsSUS>.
- [2] J. F. Gunion, H. E. Haber, G. L. Kane and S. Dawson, *Front. Phys.* **80** (2000) 1.
- [3] A. Dobado, M. J. Herrero and S. Penaranda, *Eur. Phys. J. C* **17** (2000) 487 [[hep-ph/0002134](#)]
- [4] L. J. Hall, R. Rattazzi and U. Sarid, *Phys. Rev. D* **50** (1994) 7048; M. S. Carena, D. Garcia, U. Nierste and C. E. M. Wagner, *Nucl. Phys. B* **577** (2000) 88 [[arXiv:hep-ph/9912516](#)].
- [5] W. Celmaster and R. J. Gonsalves, *Phys. Rev. D* **20** (1979) 1420.
- [6] A. H. Hoang, A. Jain, I. Scimemi and I. W. Stewart, *Phys. Rev. Lett.* **101** (2008) 151602 [[arXiv:0803.4214 \[hep-ph\]](#)]; A. H. Hoang, [arXiv:1412.3649 \[hep-ph\]](#).
- [7] K. G. Chetyrkin, J. H. Kuhn, A. Maier, P. Maierhofer, P. Marquard, M. Steinhauser and C. Sturm, *Phys. Rev. D* **80** (2009) 074010 [[arXiv:0907.2110 \[hep-ph\]](#)].
- [8] S. Moch *et al.*, [arXiv:1405.4781 \[hep-ph\]](#).
- [9] Tevatron Electroweak Working Group [CDF and D0 Collaborations], [[arXiv:1407.2682 \[hep-ex\]](#)]; V. Khachatryan *et al.* [CMS Collaboration], *Phys. Rev. D* **93** (2016) no.7, 072004 [[arXiv:1509.04044 \[hep-ex\]](#)]; M. Aaboud *et al.* [ATLAS Collaboration], *Phys. Lett. B* **761** (2016) 350 [[arXiv:1606.02179 \[hep-ex\]](#)].

- [10] M. L. Mangano, T. Plehn, P. Reimitz, T. Schell and H. S. Shao, *J. Phys. G* **43** (2016) no.3, 035001 [arXiv:1507.08169 [hep-ph]].
- [11] D. de Florian *et al.* [LHC Higgs Cross Section Working Group Collaboration], [arXiv:1610.07922 [hep-ph]].
- [12] V. P. Spiridonov, Report No. INR P-0378, Moscow, 1984.
- [13] T. Appelquist and J. Carazzone, *Phys. Rev. D* **11** (1975) 2856.
- [14] W. Bernreuther and W. Wetzel, *Nucl. Phys. B* **197** (1982) 228 [Erratum-ibid. B **513** (1998) 758].
- [15] K. G. Chetyrkin, B. A. Kniehl and M. Steinhauser, *Nucl. Phys. B* **510** (1998) 61 [arXiv:hep-ph/9708255].
- [16] R. Harlander, L. Mihaila and M. Steinhauser, *Phys. Rev. D* **72** (2005) 095009; [arXiv:hep-ph/0509048]. A. V. Bednyakov, *Int. J. Mod. Phys. A* **22** (2007) 5245 [arXiv:0707.0650 [hep-ph]]; A. Bauer, L. Mihaila and J. Salomon, *JHEP* **0902** (2009) 037 [arXiv:0810.5101 [hep-ph]].
- [17] D. Kunz, L. Mihaila and N. Zerf, *JHEP* **1412** (2014) 136 [arXiv:1409.2297 [hep-ph]].
- [18] A. V. Bednyakov, *Int. J. Mod. Phys. A* **25** (2010) 2437 [arXiv:0912.4652 [hep-ph]].
- [19] D. Noth and M. Spira, *JHEP* **1106** (2011) 084 [arXiv:1001.1935 [hep-ph]]; D. Noth and M. Spira, *Phys. Rev. Lett.* **101** (2008) 181801 [arXiv:0808.0087 [hep-ph]].
- [20] L. Mihaila and C. Reisser, *JHEP* **1008** (2010) 021 [arXiv:1007.0693 [hep-ph]].
- [21] D. Kunz, PhD Thesis, Karlsruhe Institute of Technology, 2015.
- [22] H. E. Haber, *Calif. U. Santa Cruz - SCIPP-94-039* (94/12,rec.Jan.95) 16 p [hep-ph/9501320].
- [23] P. Nogueira, *J. Comput. Phys.* **105** (1993) 279
- [24] T. Seidensticker, hep-ph/9905298.
- [25] A. I. Davydychev and J. B. Tausk, *Nucl. Phys. B* **397**, 123 (1993).
- [26] J. A. M. Vermaseren, [arXiv:math-ph/0010025].
J. Kuipers, T. Ueda, J. A. M. Vermaseren and J. Vollinga, *Comput. Phys. Commun.* **184** (2013) 1453 [arXiv:1203.6543 [cs.SC]].
- [27] R. V. Harlander, L. Mihaila and M. Steinhauser, *Phys. Rev. D* **76** (2007) 055002 [arXiv:0706.2953 [hep-ph]].

- [28] I. Jack, D. R. T. Jones, S. P. Martin, M. T. Vaughn and Y. Yamada, Phys. Rev. D **50** (1994) R5481 [hep-ph/9407291].
- [29] T. Hermann, L. Mihaila and M. Steinhauser, Phys. Lett. B **703** (2011) 51 [arXiv:1106.1060 [hep-ph]].
- [30] A. Sirlin and R. Zucchini, Nucl. Phys. B **266** (1986) 389.
- [31] E. Bagnaschi, G. F. Giudice, P. Slavich and A. Strumia, JHEP **1409** (2014) 092 [arXiv:1407.4081 [hep-ph]].
- [32] M. Steinhauser, Comput. Phys. Commun. **134** (2001) 335 [hep-ph/0009029].
- [33] 2016 Particle Data Group average, `pdg.lbl.gov`.
- [34] S. S. AbdusSalam *et al.*, Eur. Phys. J. C **71** (2011) 1835 [arXiv:1109.3859 [hep-ph]]; B. C. Allanach, A. Bednyakov and R. Ruiz de Austri, Comput. Phys. Commun. **189** (2015) 192 [arXiv:1407.6130 [hep-ph]];
- [35] D. Francescone, S. Akula, B. Altunkaynak and P. Nath, JHEP **1501** (2015) 158 [arXiv:1410.4999 [hep-ph]].
- [36] K. G. Chetyrkin, J. H. Kuhn and M. Steinhauser, Comput. Phys. Commun. **133** (2000) 43 doi:10.1016/S0010-4655(00)00155-7 [hep-ph/0004189].
- [37] L. N. Mihaila, J. Salomon and M. Steinhauser, Phys. Rev. Lett. **108** (2012) 151602 [arXiv:1201.5868 [hep-ph]]; L. N. Mihaila, J. Salomon and M. Steinhauser, Phys. Rev. D **86** (2012) 096008 [arXiv:1208.3357 [hep-ph]]; K. G. Chetyrkin and M. F. Zoller, JHEP **1206** (2012) 033 [arXiv:1205.2892 [hep-ph]]; A. V. Bednyakov, A. F. Pikelner and V. N. Velizhanin, Phys. Lett. B **722** (2013) 336 [arXiv:1212.6829 [hep-ph]].
- [38] P. M. Ferreira, I. Jack and D. R. T. Jones, Phys. Lett. B **387** (1996) 80 [hep-ph/9605440].
- [39] S. P. Martin and D. G. Robertson, Comput. Phys. Commun. **174** (2006) 133 [hep-ph/0501132].